Distinct pathways of neural coupling for different basic emotions

Marco Tettamanti[1], Elena Rognoni[2], Riccardo Cafiero[3], Tommaso Costa[2], Dario Galati[2], Daniela Perani[1,3,*]

[1]Department of Nuclear Medicine and Division of Neuroscience, Scientific Institute San Raffaele, Milano, Italy; [2]Department of Psychology, University of Turin, Torino, Italy; [3]Faculty of Psychology, Vita-Salute San Raffaele University, Milano, Italy.

[*] Address for Correspondence:

Prof. Daniela Perani, MD, Vita-Salute San Raffaele University and Scientific Institute San Raffaele, Via Olgettina 60, I-20132 Milano, Italy, Tel ++39-02-26432224, Fax + +39-02-26415202; Email: perani.daniela@hsr.it

ABSTRACT

Emotions are complex events recruiting distributed cortical and subcortical cerebral structures, where the functional integration dynamics within the involved neural circuits in relation to the nature of the different emotions are still unknown. Using fMRI, we measured the neural responses elicited by films representing basic emotions (fear, disgust, sadness, happiness). The amygdala and the associative cortex were conjointly activated by all basic emotions. Furthermore, distinct arrays of cortical and subcortical brain regions were additionally activated by each emotion, with the exception of sadness. Such findings informed the definition of three effective connectivity models, testing for the functional integration of visual cortex and amygdala, as regions processing all emotions, with domain-specific regions, namely: i) for fear, the frontoparietal system involved in preparing adaptive motor responses; ii) for disgust, the somatosensory system, reflecting protective responses against contaminating stimuli; iii) for happiness: medial prefrontal and temporoparietal cortices involved in understanding joyful interactions. Consistently with these domain-specific models, the results of the effective connectivity analysis indicate that the amygdala is involved in distinct functional integration effects with cortical networks processing sensorimotor, somatosensory, or cognitive aspects of basic emotions. The resulting effective connectivity networks may serve to regulate motor and cognitive behavior based on the quality of the induced emotional experience.

KEYWORDS: amygdala, DCM, effective connectivity, emotions, fMRI.

1. INTRODUCTION

Early neurobiological models of emotion assumed that all variety of emotions would be generated by a single specialized neural system, namely the limbic system, which links different, closely interconnected subcortical structures with higher order neocortical structures (MacLean, 1949; 1952; 1970). This notion has been fundamentally revised by contemporary neurobiological approaches, in which emotions are not defined as forming a unitary functional domain clearly distinct from cognition. Rather, raw affects – i.e. propositional forms of consciousness comprising brain and bodily processes – are thought to be turned into emotions through cognition (Panksepp, 2008). More in general, different basic emotions (Ekman, 1999) are thought to have specific psycho-behavioral correlates and to result from the integration of several functional components, including motivational, perceptual/sensory, cognitive processes (attention, memory, appraisal, and re-appraisal), motor behavior (action tendency), physiological changes, and subjective feelings (Gray, 1994; Scherer, 2000).

Recent meta-analyses of neuroimaging data strongly support the view that different emotions involve distinct arrays of cortical and subcortical structures that could instantiate these emotion-specific psycho-behavioral correlates (Murphy et al., 2003; Phan et al., 2002; Phan et al., 2004; Wager et al., 2003). More specifically, compelling evidence suggests that the insula/operculum and the basal ganglia respond more strongly to disgust, that happiness and sadness elicit stronger responses in the medial prefrontal cortices, and that the amygdala responds more strongly to fear but also to several other emotions (Murphy et al., 2003). There is also evidence of brain regions that are comparably activated by all emotions (Wager et al., 2008). Of particular relevance is the observation that the processing of emotional cues induces an increase of neural activity in perceptual areas, such as in voice-sensitive cortices in the superior temporal sulcus for emotional prosody (Ethofer et al., 2006), and in the extrastriate cortex (Morris et al., 1998)

or the fusiform gyrus (Breiter et al., 1996; Lane et al., 1997; Lang et al., 1998) in response to visual input. It has been proposed that these enhanced perceptual activations could be mediated by a modulatory feedback from the amygdala via excitatory projections (Dolan et al., 1996; Liu et al., 1999; Mayberg et al., 1999; Morris et al., 1999; Morris et al., 2002; Phelps and LeDoux, 2005; Vuilleumier et al., 2003). Such modulatory effects have a clear adaptive significance: as salient stimuli are detected, additional perceptual and attentional resources are allocated in order to process these stimuli more deeply. This emotional activation may allow the shift to specific motivational priorities and behavioral plans.

Thus, it seems that each individual emotion recruits a set of interacting subcortical and cortical regions that form specialized, distributed neural pathways. However, it is not completely understood whether the involved neural circuits consistently reflect the salient features of the different kind of emotions and how these neural systems integrate and modulate incoming information. The present event-related fMRI study aimed to investigate how the observation of video-clips inducing different basic emotions modulates the neural activity and the effective connectivity among regions selectively involved and activated in the emotional processing. Four basic emotions – i.e. fear, disgust, sadness, and happiness – were induced by film stimuli depicting scenarios containing the structure of each emotion antecedents already identified in previous studies (Boucher, 1983; Frijda, 1986; Galati and Sciaky, 1995; Scherer, 1988), thereby allowing to clearly differentiate each basic emotion without confounds among conditions. The main goals of this study were:

(i) To identify with a General Linear Model (GLM) analysis, as a measure of functional specialization, the common neural systems that respond to all emotional information derived from visual input, regardless of its specific content, and the neural systems that selectively respond to each individual basic emotion examined. To this aim, we adopted a whole-brain analysis, complemented by specific *a priori* hypotheses for conjointly activated brain regions (i.e. amygdala, extrastriate cortex, and fusiform gyrus),

and for brain regions associated with sensory, motor, and cognitive functions and responding selectively to either disgust (insula/operculum and basal ganglia), sadness and happiness (medial prefrontal cortex), or fear stimuli (fronto-parietal cortex).

(ii) Based on the results of the GLM analysis, to investigate with Dynamic Causal Modeling (DCM), as a measure of functional integration, how the different emotions modulate neural interactions between common brain regions processing all emotions, such as the amygdala, and the brain regions underlying the processing of domain-specific sensory, motor, and cognitive features.

In particular, we defined three different emotion-specific DCM models, based on the results of the GLM analysis showing selective anatomo-functional effects for fear, disgust and happiness, but no selective anatomo-functional effects for sadness. First, in relation to fear, a model testing for the interactions between the amygdala and fronto-parietal regions coding for action representation (Calvo-Merino et al., 2005; Decety and Grèzes, 2006), which may be crucial for the preparation of an adaptive motor response to a fearful stimulus (Grèzes et al., 2007). Second, in relation to disgust, a model testing for the interactions between the amygdala and the somatosensory cortices coding for bodily representations, compatible with the self-boundary function of disgust as mediating a rejection response that protects the body from offensive and contaminating entities (Fessler and Haley, 2006; Miller, 2004). Third, in relation to happiness, a model testing for the interactions between the amygdala and brain regions associated with mentalising and evaluating others' emotional states (Burnett and Blakemore, 2009; Lee and Siegle, in press), possibly mediating the understanding of joyful interactions between conspecifics.

2. MATERIALS AND METHODS

2.1. Participants

Nineteen right-handed (Oldfield, 1971) women voluntarily took part in the experiment (mean age 24.1 years, s.d. 5.2, range 19-39 years). A group of exclusively females was selected to control for gender differences in emotion-related brain activations and in light of stronger psychophysiological responses and subjective feelings in response to emotions in women than in men (Wager et al., 2003). Subjects were neurologically and psychiatrically healthy, unmedicated, and paired for socio-demographic characteristics and education level. A screening procedure was adopted to select the subjects: a preliminary anamnesis interview was conducted by a clinician to exclude any neurological or psychiatric disorders (SCID-I for clinical disease on 1st axis of the DSM-IV, and SCID-II for personality disorders on the 2nd axis of the DSM-IV), and a battery of personality tests (Big Five Questionnaire, Profile of Mood States, Positive Affect Negative Affect Schedule, Levels of Emotional Awareness Scale) was adopted to exclude subjects who presented outlier scores on personality dimensions concerning the affective sphere.

Subjects gave written consent to participate in the study after receiving an explanation of the procedures, according to the Declaration of Helsinki. The study was approved by the Ethics Committee of the University of Turin, Italy.

2.2. Stimuli and experimental design

Stimuli consisted of 120 video-clips (Supplementary Table 1), each 10 s long, representing different emotional scenarios of fear, disgust, sadness, and happiness, and scenarios with non emotional, neutral content (24 video-clips for each condition). The video sequences were selected from a set of stimuli prepared by our group to induce specific basic emotions. Each stimulus was extracted from commercial movies, selecting

the sequences reflecting prototypical and specific antecedents of emotion on the basis of theoretical criteria and contributions from psychology research on emotional antecedents (Boucher, 1983; Frijda, 1986; Galati and Sciaky, 1995; Scherer, 1988). Film excerpts were then edited to exclude any details that could alter the emotional quality of the target response (e.g., facial expressions of a different emotion than the target emotion). The film clips obtained were pre-tested and validated on a sample of judges (n = 30, mean age 24.7 years, s.d. 4.3, range 18-34 years). The video-clips were correctly identified with respect to the hypothesized emotion, with a stimulus recognition rate of 93.5 % for fear, 88.0 % for disgust, 84.2 % for sadness, 93.1 % for happiness, and 80.4 % for neutral. There were no significant differences in recognition rates between the experimental conditions (Fisher exact test = 6.28, P = 0.094). To evaluate the agreement between the hypothesized emotions and the emotions assigned by the judges, we calculated the Cohen's Kappa coefficient, which showed a highly significant agreement (K = 0.89, P < 0.001). Highly significant was also the χ^2 (P < 0.001) calculated with a double-entry table (expected ratings vs. ratings assigned by the judges).

A further validation was conducted to ascertain that the stimuli selected for the present fMRI study were able to actually elicit an intense emotional response: to this aim, skin conductance responses for each of the 30 judges were recorded. A repeated measures ANOVA with the five experimental conditions as a within-subject factor showed a significant main effect ($F(1.7, 41.97) = 10.5$; $P < 0.001$; $\eta^2 = 0.3$). Post-hoc paired tests revealed a significant increase in the responses elicited by emotional vs neutral stimuli (P < 0.001, Bonferroni corrected for multiple comparisons), and no significant differences between the emotion conditions.

Fear (F) sequences depicted men or animal aggressions and dangerous situations such as falling and drowning. Disgust (D) sequences depicted contamination scenarios, such as by offensive or infective agents. Sadness (S) sequences depicted scenes of

death, loss, sickness and sorrow. Happiness (H) sequences depicted meaningful interactions among subjects, such as lovers' encounters, amusement scenes and successful life's moments. Neutral (N) sequences depicted a series of routine human actions and activities devoid of emotional content (see Supplementary Material for example video-clips). All stimuli were in color, without sound, balanced in relation to the presence of human beings and number of cuts. All of the visual features that could produce any confounds on input level, such as luminance or movement, were varied across conditions.

The stimuli were presented in a jittered event-related experimental design, divided in four separate runs, each containing 6 video-clips for each condition. Stimuli were randomly assigned to the four runs both within and between subjects. Three different inter-stimulus intervals were used, corresponding to 1950 ms (n = 17), 3950 ms (n = 9), and 5750 ms (n = 5) randomized both within and between run and subjects, to maximize the hemodynamic signal sensitivity of the event-related design.

2.3. Self-report of subjective emotional experience after fMRI

In order to verify that the stimuli material was able to elicit the target emotional response in the participants of the fMRI study, the subjective emotional experience was obtained after MR scanning using a self-report consistent with both dimensional and discrete models of emotion. Subjects rated each stimulus on a 9-point Likert scale for emotional valence (from 1 for very unpleasant to 9 for very pleasant), emotional arousal (from 1 for calm to 9 for highly excited), and intensity (for each emotion, from 1 for no feeling to 9 for very intense feeling). The structure and the metric properties of the self-report scales were comparable to those previously employed to generate and validate emotional stimuli, such as film (Rottenberg et al., 2007) or affective pictures (IAPS, Lang et al., 1997).

2.4. fMRI data acquisition

MRI scans were acquired on a 3T Intera Philips body scanner (Philips Medical Systems, Best, NL) using an 8 channels-sense head coil (sense reduction factor = 2). Whole-brain functional images were obtained with a T2*-weighted gradient-echo, echo-planar sequence, using blood-oxygenation-level-dependent contrast. Each functional image comprised 30 contiguous axial slices (4 mm thick), acquired in interleaved mode, and with a repetition time of 2000 ms (echo time: 30 ms; field of view: 240 mm x 240 mm; matrix size: 128 x 128). Each participant underwent 4 functional scanning sessions. The duration of each session was 200 scans, preceded by 10 dummy scans that were discarded prior to data analysis.

We also acquired a high-resolution whole-brain structural T1 weighted scan (resolution 1mm x 1mm x 1mm) of each participant for anatomical localization and visualization of brain activations.

2.5. Data analysis

Statistical parametric mapping (SPM5, Wellcome Department of Imaging Neuroscience, London, UK) was used for slice timing, image realignment and unwarping, normalization to the Montreal Neurological Institute (MNI) standard space, smoothing by a 6 mm FWHM Gaussian isotropic kernel, and GLM statistical analysis.

We adopted a two-stage random-effects approach to ensure generalizability of the results at the population level.

2.5.1. First-level General Linear Models

At the first stage, the time series of each participant were high-pass filtered at 67 s and pre-whitened by means of an autoregressive model AR(1). No global scaling was

performed. Hemodynamic evoked responses for all experimental conditions were modeled as canonical hemodynamic response functions with the temporal and dispersion derivatives to compensate for slight variations of the BOLD signal.

For each participant, we modeled the factor condition with 4 separate sessions (5 levels: F, D, S, H and N). First-level t-Student contrasts were specified, each contrast including a weight of one for a particular regressor of interest and a weight of zero for all the other regressors. This resulted in one contrast per experimental condition and per hemodynamic basis set for each participant.

2.5.2. Second-level General Linear Model

At the second stage of analysis, the t-Student contrasts defined at the single-subject level were used to compute a within-subjects one way ANOVA assessing their significance at the group-level (n = 19 participants).

At the second-level, we then specified a series of massed univariate F contrasts, spanning the canonical hemodynamic response function and its two derivatives. In order to investigate the spatial overlap of regions displaying selective fMRI signal increases during all the types of emotional video clips, we performed a null conjunction analysis of the four contrasts in which each emotion was compared with the Neutral condition: [(F–N) conj. (D–N) conj. (S–N) conj. (H–N)]. All reported effects on this whole-brain analysis are related to voxel-level statistics, $P < 0.05$, using a family wise error (FWE) type whole-brain correction for multiple comparisons and a cluster extent threshold of greater than 5 voxels. Since no activation of the amygdala survived a whole-brain correction, Small Volume Correction ($P < 0.05$, FWE corrected) was used within this conjunction analysis to specifically test the *a priori* hypothesis of the shared activation of the amygdala irrespective of the particular emotion processed: the search volume over the amygdala was defined on an anatomical basis using the WFU Pickatlas toolbox within SPM5.

Subsequently, we investigated the specific effects for each individual emotion, by exclusively masking the contrast of a given emotion vs. the Neutral baseline with the corresponding contrasts for all the other emotions, i.e.: for Fear: [(F-N) exclusively masked by (D-N), (S-N), (H-N)]; for Disgust: [(D-N) exclusively masked by (F-N), (S-N), (H-N)]; for Sadness: [(S-N) exclusively masked by (F-N), (D-N), (H-N)]; for Happiness: [(H-N) exclusively masked by (F-N), (D-N), (S-N)]. A $P<0.05$, FWE whole-brain correction was chosen. We used a Small Volume Correction ($P < 0.05$, FWE corrected) to test for the activation of emotion-specific brain regions predicted by the extant literature (Murphy et al., 2003; see Introduction), which did not survive a whole-brain correction. These were, the basal ganglia (caudate, putamen and globus pallidus) for the specific effect of Disgust (and, as a control, for Fear, Sadness and Happiness), and the medial prefrontal cortex (MPFC) for the specific effects of Happiness and Sadness (and, as a control, for Fear and Disgust). All the significant activation clusters obtained in the above listed contrasts were inspected for emotion-specific effects by plotting the effects sizes for all effects of interest: only clusters that displayed significant and emotion-specific activity are reported.

Finally, we also performed a set of correlation analyses, in order to assess whether the specific effects for each emotion could be at least in part ascribed to individual variations in the level of valence, arousal, and intensity, as measured by the ratings reported by each subject after the fMRI scanning session. To do so, we specified a set of group-level one-sample t-tests, each including the single-subject t-Student contrasts of interest for the canonical hemodynamic response function (e.g. for Fear: [F-N]), and the corresponding covariate (e.g. for the correlation between Fear and reported valence: (valenceF – valenceN)). Both positive and negative correlations were computed, applying a $P<0.05$, FWE whole-brain correction.

2.5.3. Dynamic Causal Modeling

Based on the results of our GLM analysis showing selective effects for Fear, Disgust and Happiness, but not for Sadness (see Results), we used DCM (Friston et al., 2003) to test the hypothesis that the right amygdala showed a positive increase of coupling with the extrastriate visual cortex and with either the fronto-parietal system, the somatosensory system, or higher order cortical regions, reflecting the different type of emotion expressed by the presented video-clip stimuli:

1. For Fear, we expected a relatively stronger coupling between amygdala, extrastriate visual cortex and fronto-parietal regions, reflecting the preparation of a motor adaptive response to a fearful stimulus.

2. For Disgust, we expected a relatively stronger coupling between amygdala, extrastriate visual cortex and somatosensory brain regions, reflecting a rejection response to disgust stimuli as a protection against offensive and contaminating entities.

3. For Happiness, we expected a relatively stronger coupling between amygdala, extrastriate visual cortex and medial prefrontal and temporo-parietal brain regions that have been associated with the evaluation of others' emotions, possibly reflecting the understanding of joyful interactions between conspecifics.

In order to assess these condition-specific modulations, we specified three dynamic causal models that were characterized by the common involvement of the right amygdala (Ramy) and right inferior occipital gyrus (RIOG), as revealed by the conjunction analysis, but differed with respect to the other regions included in the models, as revealed by the specific effects of each individual emotion: 1) for Fear-DCM, the right dorsal premotor cortex (RBA6) and the right precuneus/superior parietal lobule complex (RPcn/SPL)**;** 2) for Disgust-DCM, the right thalamus (Rtha), the left insula (Lins), and the right secondary somatosensory cortex (RBA2); 3) for Happiness-DCM, the right temporo-parietal junction (RTPJ) and the right medial prefrontal cortex (RMPFC).

It must be emphasized that DCM is not an exploratory technique, but rather a confirmatory technique that relies on *a priori* hypotheses, based on independent evidence, to infer inter-regional causality effects. Furthermore, the number of brain regions that may be included in each dynamic causal model is limited in the current DCM implementation in SPM8 (maximum of 8 regions), and more specific inferences can be tested if the model space dimensions are kept to a minimum (Stephan et al., 2010). For these reasons, we decided to include a maximum of 5 brain regions for each dynamic causal model. In case of bilateral involvement of any given brain region, we only included the right hemispheric side, reflecting the side of significant activation in the amygdala in the null conjunction GLM analysis. Only one left hemispheric regions was included, i.e. Lins in Disgust-DCM, due to the lack of corresponding right hemispheric activation.

First, we defined for each participant two General Linear Models that were specifically designed to encompass the requirements of the intended DCM analysis. The first GLM matrix (dcm-GLM) was entered during DCM model specification and included a separate regressor representing all stimuli of all conditions (ALL) and additional regressors for the individual conditions F, D, S, H and N. To avoid the issue of colinearity between regressors within dcm-GLM, which would interfere with the definition and extraction of volumes of interest, we also specified a second GLM matrix (voi-GLM), that only included the regressors for the five individual conditions but no ALL regressor. The voi-GLM matrix was only used to extract volumes of interest and was not directly entered during DCM model specification.

In both the voi-GLM and the dcm-GLM, the time series of each participant were high-pass filtered at 67 s and pre-whitened by means of an autoregressive model AR(1). Evoked responses were modeled with the canonical hemodynamic response function, time-locked to the onset of video-clip presentation. We modeled the 4 functional scanning sessions as one single concatenated session and we included (4-1) additional constant

regressors, each with values of 1 for the scans of one session and 0 for the other scans, to account for the separate functional scanning sessions.

Within the voi-GLM model of each participant, we computed one t-Student contrast defining the main effect of all emotion conditions vs the Neutral baseline [(F+D+S+H)-N]. This contrast was used to identify subject-specific volumes of interest for the brain regions included in the three dynamic causal models. Subject-specific volumes of interest were defined through a small volume correction procedure. First, we computed the main effect contrast. We then defined spherical volumes (radius = 6 mm) around the group-level coordinates of the brain regions included in the three models (see Tables 1 and 2), and extracted the maximum activation peak for each subject. We also checked that the subject-specific coordinates identified through this procedure actually corresponded to the same anatomical location represented by the group-level coordinates. We extracted spherical volumes of interest of 6-mm radius centered on the identified subject-specific coordinates. The volumes of interest were corrected for the effects of interest (omnibus F-test), such that it was not biased toward any particular experimental conditions, but instead included the information relative to the stimuli of all conditions.

We adopted a two-stage random-effects approach for the DCM analysis. At the single-subject level, we implemented Fear-DCM, Disgust-DCM, and Happiness-DCM, based on dcm-GLM. In all three DCM models the ALL regressor provided direct input to RIOG. F, D, S, H, and N were then allowed to separately modulate all the connections in the three tested models, whereby in all the three DCM models all the areas were connected to all the other areas (fully connected models).

At the second-level, we performed classical statistical analyses using R 2.10 (www.r-project.org) – corresponding to second-level random-effects analyses – on the arithmetic (non-Bayesian) means of the first-level modulatory connection-strengths of the three DCM models. For the modulatory connection strengths, we first used a Lilliefors

(Kolmogorov-Smirnov) normality test to check the normality of the distribution of the values pertaining to each connection. Given a highly preponderant normal distribution, we then applied throughout parametric one-tailed tests of means (t-Student). For the modulatory effects, we first tested, for each condition taken alone (F, D, S, H, and N), the alternative hypothesis that each connection strength was significantly greater than zero (one-tailed test for positive modulations) or significantly smaller than zero (one-tailed test for negative modulations). We then performed pairwise comparisons between the experimental conditions, by testing the alternative hypothesis of: 1) a stronger effect for Fear vs. each of the other 4 conditions (within Fear-DCM); 2) a stronger effect for Disgust vs. each of the other 4 conditions (within Disgust-DCM); 3) a stronger effect for Happiness vs. each of the other 4 conditions (within Happiness-DCM). To account for the number of tested connections (12 connections in both Fear-DCM and Happiness-DCM, and 20 connections in Disgust-DCM), we calculated False Discovery Rate (FDR) (Benjamini and Hochberg, 1995) corrected ($P<0.05$) alpha values (Table 3).

3. RESULTS

3.1. Behavioral results

To evaluate the agreement between the hypothesized emotions and the emotions assigned by the fMRI study participants, we calculated the Cohen's Kappa coefficient, which showed a highly significant agreement ($K = 0.74$, $P < 0.001$). Highly significant was also the χ^2 ($P < 0.001$) calculated with a double-entry table (expected ratings vs. ratings assigned by the participants).

Furthermore, in order to verify if the subjective emotional responses were actually differentiated in relation to the different basic emotions, subjective post-scan ratings for valence, arousal, and intensity were each compared by a repeated measures ANOVA including the within-subject factor Condition (5 levels: F, D, S, H, N). The Huynh-Feldt correction on degrees of freedom was adopted when the sphericity assumption was violated. Post-hoc analyses were done using paired t-Student tests, Bonferroni-corrected for multiple comparisons. The main effect of Condition was highly significant for all three dimensions: valence: $F(2.3, 44.1) = 975.2$, $P < 0.001$, $\eta^2 = 0.98$; arousal: $F(4, 76) = 151$, $P < 0.001$, $\eta^2 = .089$; intensity: $F(4, 76) = 204.5$, $P < 0.001$, $\eta^2 = 0.91$.

With respect to valence (mean values (s.d.): F: 1.84 (0.45); D: 1.55 (0.27); S: 1.83 (0.36); H: 7.55 (0.47); N: 4.62 (0.57)), there was a significant difference ($P < 0.001$) between all experimental conditions, except between F and S, with the ratings for N video-clips receiving a mid pleasantness score.

With respect to arousal (F: 5.30 (1.15); D: 6.58 (1.06); S: 4.55 (1.01); H: 5.11 (0.97); N: 1.59 (0.31)), N video-clips received a lower score and D video-clips a higher score than all the other conditions (both $P < 0.001$); F differed from S ($P < 0.01$) but not from H.

Also with respect to intensity (F: 6.42 (0.99); D: 6.84 (1.01); S: 6.19 (0.92); H: 6.30 (0.82); N: 1.96 (0.41)), N video-clips received a lower score than all the other conditions

(both $P < 0.001$), whereas there were no significant differences between the four emotional conditions.

These results confirmed that each emotional condition actually elicited subjective responses clearly differentiated both at the categorical and at the dimensional level.

3.2. fMRI results

The conjunction analysis revealed a set of activations prevalently located in the right hemisphere (Table 1 and Figure 1A). More specifically, we observed an overlap of activation across all the four basic emotions compared to Neutral in the right amygdala, in the right supramarginal gyrus, in the right postcentral gyrus, in the left inferior and middle temporal gyri, in the left fusiform gyrus, and, bilaterally, in the superior parietal lobules and in the inferior occipital gyri. The right cerebellum (at the level of the crus I and VI lobules) was also activated.

The analysis of the specific effects for each individual emotion revealed the involvement of additional emotion-specific neural systems for three emotions, i.e. Fear, Disgust and Happiness, but not for Sadness.

Fear specific effects (Table 2A and Figure 1B) were found in the frontal, parietal and occipital cortex, including in particular the right superior frontal gyrus, and bilaterally the precuneus/superior parietal lobule complex and the associative occipital cortex (middle occipital gyrus, fusiform gyrus and lingual gyrus).

Disgust (Table 2B and Figure 1C) activated several cortical and subcortical regions, mostly bilaterally, including: the inferior frontal gyrus, both in the pars triangularis and pars opercularis, the precentral gyrus and the postcentral gyrus , the inferior parietal lobule, the inferior temporal gyrus, and a large cluster in the precuneus, cuneus, lingual and calcarine gyri. Moreover, we found bilateral activations in the cerebellum (crus I,II, and VI lobules), in the amygdala and thalamus. In addition, Disgust elicited activation increases in other left

hemispheric regions, including limbic structures such as the insula and the middle cingulate cortex, and also the superior frontal gyrus, the middle and superior temporal gyri, and the middle and superior occipital gyri. Notably, no Disgust-specific effects were found in the basal ganglia, as would have been predicted by the extant literature.

Sadness (Table 2C) was not associated with any specific activations in addition to those revealed by the conjunction analysis. No specific activations were found even based on an *a priori* hypothesis for the medial prefrontal cortex.

Happiness (Table 2D and Figure 1D) elicited right hemispheric activations in the medial prefrontal cortex and in the superior temporal gyrus / temporo-parietal junction. Bilateral activations were found in the middle temporal gyrus.

Finally, the analyses testing for a correlation between the specific effects for each emotion and the subjective valence, arousal, and intensity ratings reported by each subject after the fMRI scanning session, did not reveal any significant positive or negative effects. This indicates that the specific effects for each emotion reported above were not confounded by subjective variations in the reported quality and quantity of the emotional response.

3.3. DCM results

The aim of the DCM analysis was to examine how common and domain-specific brain regions interact with each other, and how the strength and directionality of such interactions is differentially modulated by the four basic emotions investigated here.

At the general level, all the three tested dynamic causal models provided results in agreement with the specified *a priori* hypotheses. We observed that, in line with our predictions, the experimental condition of interest within each of the three specified models (F for Fear-DCM; D for Disgust-DCM; H for Happiness-DCM) induced positive modulations, i.e. increases of connection strengths, and no negative modulations, i.e.

decreases of connection strengths. This did not always hold true for the other experimental conditions within each of the three models (D, S, and H for Fear-DCM; F, S, and H for Disgust-DCM; F, D, and S for Happiness-DCM), which displayed both positive and negative modulations, many of which were not significant. Notably, the N condition mostly induced negative or non-significant modulations within the three specified models, indicating a reduced functional integration in brain systems related to emotion processing, consistent with the lack of emotional content in N videos.

In other words, at such a general level (i.e. considering each dynamic causal model as a whole, without consideration of the significance and directionality of the individual inter-regional effects within each model), we observed the expected pattern of higher functional integration for F within Fear-DCM, for D within Disgust-DCM, and for H within Happiness-DCM.

At a greater level of detail, the Fear-DCM model was associated with an increase of modulatory strengths that was specific for the F condition in the connection RIOG->RPcn/SPL (compared to all the other four conditions) and in the connections RIOG->RBA6 and RBA6->RPcn/SPL (compared to all other conditions except for D), compatible with our hypothesis of an involvement of motor representations and action preparation in fear processing (Table 3A and Figure 2A). Other connections within Fear-DCM showed F-specific effects but only compared to S and H (RPcn/SPL->RIOG, RBA6->RIOG) or to H alone (Ramy->RPcn/SPL). It is interesting to note, that the backward connections from fronto-parietal regions to the amygdala were not significantly modulated, indicating a predominantly forward modulatory role of the amygdala onto the domain-specific brain system. Also of interest is the fact that the RPcn/SPL received F-specific modulations from all the other three regions included in the model, suggesting that the RPcn/SPL may play a role in the integration of core emotional information extracted by visual input with action representations.

The Disgust-DCM model showed an increase of modulatory strengths in the connections RIOG->Lins and Ramy->Lins, which was significantly greater for D compared to all the other four conditions (Table 3B and Figure 2B). Crucially for our hypothesis of an involvement of a somatosensory system as a reaction to disgusting stimuli, specific modulation increases for D were found for three of the four connections toward RBA2, namely those originating from RIOG, Ramy and Lins. In the case of RIOG->RBA2 and Ramy->RBA2, the effects was greater for D compared to all the other conditions; in the case of Lins->RBA2, the effect for D was greater than the effects for F, S and H but not significantly greater than the effect for N. Backward connections from RBA2 also showed specific modulation increases for D, namely the connection RBA2->RIOG (compared to all the other four conditions) and the connection RBA2->Lins (compared to F and S). Within Disgust-DCM, RBA2 thus seems to play a pivotal role in integrating and regulating the flow of information between core emotion processing regions and somatosensory ares. Other connections within Disgust-DCM showed D-specific effects compared to at least two of the other conditions, including RIOG->Ramy, Ramy->RIOG, Rtha->Lins, and Lins->RIOG. It is interesting to note, that by analogy with a comparable observation for Fear-DCM, no backward connections from somatosensory regions to the amygdala were significantly modulated, again pointing to a predominantly forward modulatory role of the amygdala onto a domain-specific brain system.

Within the Happiness-DCM model, H elicited significantly greater increases of modulatory strengths compared to D and N in the connection RIOG->RTPJ, compared to D for the connection Ramy->RTPJ, and, crucially for our hypothesis, compared to F and D in the connection RMPFC->RTPJ (Table 3C and Figure 2C). Thus, RTPJ appears to be a region of convergence of the information exchanged between the areas constituting the Happiness-DCM model. Similar to the other two DCM models, the amygdala exerted significant modulatory effects in outward but not in backward connections, once again

pointing to its predominantly forward modulatory role in the context of visual emotion processing.

4. DISCUSSION

This fMRI study investigated in healthy women the neural responses during passive viewing of video-clips of four distinct basic emotions and a neutral control condition, and examined the effective connectivity within neural networks linking the amygdala and the extrastriate visual cortex with other brain regions involved in the processing of the sensorimotor, perceptual-somatic, and cognitive-social components of emotions. Importantly, the present study did not specifically focus on the recognition of emotions based on facial expressions, an aspect deeply investigated in a number of previous studies (Adolphs, 2002; Eimer and Holmes, 2007; Loughead et al., 2007; Streit et al., 1999), but rather on the dynamic processing of emotions under ecological, passive viewing conditions, with emotional-rich videos extracted from commercial movies. Previous works have focused on differences between passive viewing and explicit evaluation, like rating the affective response, outlining no significant differences due to the task in brain regions involved in emotion recognition (Hutcherson et al., 2005). On the contrary, the dynamic presentation of emotional stimuli may enhance recognition accuracy (Ambadar et al., 2006) and arousal rates (Weyers et al., 2006), resulting in an increased activation of sensory cortices related to the modality of stimuli presentation (Adolphs, 2002, Ethofer et al., 2009).

4.1. Discussion of experimental setting and behavioral results

The analysis of the subjective post-MR emotional ratings showed that the four emotional video-clips categories were clearly differentiated from the Neutral condition, in terms of valence, arousal, and intensity. This is consistent with the view that the emotional stimuli were properly designed to induce a measurable emotional response. Importantly, the four emotional conditions did not significantly differ from each other in terms of intensity, thus ruling out the possibility that the observed differences in terms of brain

activation and connectivity might be due to spurious effects of perceptual salience. Vice versa, significant differences were observed between the four emotional conditions in terms of valence, with effect directions matching the emotional content of each category, i.e. scores indicating pleasantness for H video-clips and unpleasantness for F, D, and S video-clips. With respect to arousal scores, the differences between emotional conditions appear to match at least in part the distinction between emotions involving behavioral activation (F, D, H) vs behavioral inhibition (S). In addition to these dimensional results, our behavioral data also show that there was a high agreement between the *a priori* categorization of the video-clips according to the five experimental conditions and the categories assigned by the experimental subjects. Both the dimensional and categorical results thus provide evidence that the stimulus material was adequate for investigating the specific basic emotional systems of interest with fMRI.

4.1.1 Limitations of the present study

While we have emphasized the importance of investigating the neural responses to emotions under ecological, passive viewing conditions, through the employ of video-clips extracted from commercial movies, we also acknowledge that the increased visual complexity of video stimuli, compared to static pictures, makes it more difficult to carefully control for all irrelevant psychophysical, visual dimensions that may confound the emotional response. Future studies may circumvent these problems, e.g. by employing filtered or synthesized video materials. In the present study, we have done our best to match the experimental stimuli and the baseline Neutral stimuli with respect to gross perceptual components, such as the presence of human action scenes and human faces. Accordingly, all the reported emotion-specific activation effects were computed by subtracting the Neutral condition from the emotion conditions of interest (F, D, S, H), thus

at least roughly controlling for the general, emotion-unrelated, perceptual features included in the experimental stimuli.

Furthermore, while we have underlined that the lack of significant correlations with subjective ratings indicates that the reported activation effects were not confounded by subjective variations in the reported quality and quantity of the emotional response, it may also be argued that, particularly with respect to valence and arousal, this weakens the interpretation of the activations in terms of emotion-specific neural responses. However, higher valence or arousal subjective scores do not necessarily imply a more specific or genuine response to the induced emotion, but may also relate to individual differences in the conscious evaluation of the emotional responses. More sensitive measures and analytic strategies may be adopted by future studies, such as the use of a parametric approach to correlate stimulus-specific behavioral indices or physiological responses (e.g. skin conductance) with fMRI activations. This was not possible in the present study, where the emphasis was on average emotion-specific neural responses, with comparably small within-condition stimulus variance. Indeed, the 24 video-clips in each set differed in content (see Supplementary Table 1) but were highly similar in terms of valence, arousal, and intensity, as can be inferred from the standard deviations, which were small compared to the mean values (see section 3.1).

As a further potential limitation of the present study, it must be noted that a group of exclusively female healthy volunteers was included in the present fMRI study. This was done in order to avoid the problem of gender differences in emotion-related brain activations (Wager et al., 2003), and to maximize the activations induced by subjective feeling responses in our passive viewing task. This however implied that the results presented here cannot be extended to the general population, and further studies will be required to clarify the gender-specific recruitment of sensorimotor and cognitive systems for the processing of basic emotions.

4.2. Discussion of fMRI and DCM data

The first objective of the fMRI data analysis was to identify the neural structures that conjointly responded to all the emotions investigated. The conjunction analysis indeed showed that a distributed array of brain regions subserves the processing of all kind of emotional stimuli investigated here compared to a neutral condition (Table 1 and Figure 1A). Such distributed neural array included the right amygdala, associative occipital and temporal regions, and the cerebellum, consistently with a recent meta-analysis focusing on the neural reference space for emotions (Wager et al., 2008). This set of brain structures is thought to instantiate emotions and related affective space (Feldman Barrett et al, 2007). The amygdala has been shown to enhance the occipital and ventral stream activity (Shuler and Bear, 2006; Freese and Amaral, 2005; Vuilleumier et al., 2004). The cerebellum is extensively interconnected with fronto-limbic regions (Middleton and Strick, 2001) and is involved in emotional processing, as revealed by deep cerebellar nuclei stimulation, which induces activity in the mesolimbic areas (Heath et al., 1978) and even causes profound rage states (Heath et al., 1974), and by cerebellar lesions leading to emotional disregulation (Schmahmann and Sherman, 1998).

In contrast to the meta-analysis by Wager and colleagues (2008), our conjunction analysis failed to reveal activations in several subcortical structures (periaqueductal gray, ventral tegmental area, hypothalamus), which have been found especially in animal studies, possibly due to the higher spatial resolution of these studies compared to human fMRI studies. The conjunction analysis also did not reveal activations in other brain structures implicated in the processing of emotions (Pessoa, 2008; Phan et al., 2002; Wager et al., 2008), such as the hippocampus, the thalamus, the orbitofrontal cortex, the dorsomedial prefrontal cortex, the cingulate cortex, or the superior temporal sulcus/gyrus. Nevertheless, it must be noted, that the stringent criteria imposed by the kind of null

conjunction analysis performed here only yielded activations in those brain structures displaying a significant comparable effect in all the emotional conditions when contrasted to the Neutral baseline. In other words, if a particular brain structure was either not significantly activated in even just one condition or not activated in an overlapping manner compared to the other three conditions, then the corresponding effect would not show up in the conjunction analysis. In agreement with such an explanation, activations in some of the aforementioned brain regions were indeed revealed by the statistical contrasts looking for the specific effects for each individual emotion, as shown in the Results and discussed below.

The rest of our discussion concentrates on the other main objectives of the present study, which consisted, on the one hand, in identifying the functionally specialized brain regions for each individual emotion and, on the other hand, in analyzing the domain-specific functional integration within neural networks linking the amygdala and visual areas with either fronto-parietal, somatosensory or cognitive brain regions. Also for the analysis of functional specialization and integration effects we applied stringent criteria: in particular, by using an exclusive masking procedure, we only focused on activation effects for a given basic emotion that were not significant for any of the other basic emotions considered here. Thus, if a particular brain structure was activated in an overlapping manner by two or more basic emotions, then the corresponding effect would not show up in the analysis of the specific effects for each individual emotion. As a consequence, only brain regions responding selectively to a single basic emotions were included in the DCM analysis. We have chosen such a stringent approach in order to highlight truly specific neural representations and networks. This crucial aspect also helps to explain why, as we will describe in more details below, previous works using less stringent criteria generally found more distributed activations for the different basic emotions.

We recognize that our approach for measuring the patterns of functional integration specific to each emotion has several limitations. In order to comply with both the technical limitations of DCM and the increasing degree of inferential complexity with increasing model size, we have chosen to restrict model size to a maximum of 5, mainly right hemispheric, brain regions for each dynamic causal model. While our approach allowed us to test for specific *a priori* experimental hypotheses, the defined models may represent an oversimplification with respect to actual brain mechanisms. More specifically, there is a clear disparity between the relatively large number of brain regions being either conjointly of specifically activated by the four basic emotions and the small number of regions included in the 3 dynamic causal models. Among the regions conjointly activated (Table 1), we have chosen to focus on RIOG and Ramy for the DCM analysis, as representative brain structures of a neural system for conscious encoding of visual stimuli with an emotional content. Clearly, however, other conjointly activated brain regions excluded from our DCM analysis, such as the right inferior temporal or superior parietal cortices, may be essential for the visual encoding process and, if included in the dynamic causal models, may have provided important, complementary evidence or even altered the connectivity result in many respects. A further oversimplification may be the restriction to just 2 or 3 domain-specific brain regions to be included in the dynamic causal models for Fear (Table 2A) and Disgust (Table 2B), respectively. Our choice to focus on, respectively, a brain system subserving adaptive motor responses for Fear, and a brain system subserving somatic responses for Disgust, may only represent one valid alternative among others, one that we believe is confidently predicted and supported based on the extant literature. Future studies, possibly employing other more flexible effective connectivity techniques such as Granger causality (Roebroeck et al., 2005), may be necessary to provide a less simplified picture than the one reported here. For instance, the processing of basic emotions may not only rely on domain-specific segregated systems but also largely on

differences in the functional interactions between commonly recruited brain regions. Nevertheless, we are confident that, even considering these notes of caution, our study represents a valid exploratory starting point for the still largely unexplored issue of the distributed neural processing of emotions.

4.3. Fear

We showed that fear is specifically associated with activation foci in frontal, parietal, and occipital areas (Table 2A and Figure 1B). Traditionally, fear has been tightly associated with activity of the amygdala, a coupling that has been supported by extensive animal research (LeDoux, 2000), and in humans by functional neuroimaging (Murphy et al., 2003). More recent works brought evidence that fear may not be specifically represented in the amygdala. Atkinson et al. (2007) observed that a patient suffering from bilateral amygdala lesions was still able to recognize fear through static or dynamic bodily expressions. Tsuchiya and colleagues (2009) made the observation that bilateral amygdala lesions do not compromise fear recognition: the role of the amygdala may rather reflect appraisal-like evaluations of the biological relevance of stimuli and the explicit judgment of emotions. This lack of specificity is also in agreement with the present findings in the conjunction analysis showing a consistent activation of the right amygdala for all the emotional conditions.

Stark et al. (2007) investigated fear and disgust picture rating and found fear specific activations in the middle and superior occipital gyri and in the fusiform gyrus, comparable to those reported here. In contrast to the present study, however, they also found fear specific activations in the inferior frontal gyrus, cingulate cortex and middle temporal gyrus. An activation in the precuneus was also present, although at a different stereotaxic location than the one reported here. A different study focusing on fearful dynamic body expressions also showed fear specific activations in the left precuneus that were more

overlapping to our activations, but, at odd with our results, also showed temporal activations (Grèzes et al., 2007). De Gelder and colleagues (2004) contrasted fearful bodily expressions compared to neutral ones and found activations – in addition to the bilateral fusiform gyrus and inferior frontal gyrus, and the right amygdala – in the right precuneus and in the right superior frontal gyrus (BA6), with close similarity to our findings.

The fronto-parietal network activated by fearful stimuli points to processes of action representation and action preparation (Calvo-Merino et al., 2005; Decety and Grèzes, 2006), but It is also possible that other processes, such as attentional or control functions, may be involved. Closely matching activation coordinates in the frontal premotor cortex and the superior parietal lobule have been particularly found in previous works on motor imagery (Guillot et al., 2008; Hanakawa et al., 2003; Malouin et al., 2003). Even though we do not assume that the observation of fearful video-clips engaged explicit motor imagery, an implicit form of mental action simulation and preparation may be crucial for the selection of an adaptive behavioral response needed to cope with dangerous events (Grèzes et al., 2007). This idea is in line with a number of studies on the effects of fear on the motor system. Fearful stimuli elicit shorter reaction times than control stimuli and this could reflect the fast implicit preparation of action in response to danger (Flykt, 2006). Defensive mechanisms such as the startle reflex undergo a potentiation during the exposure to actual threat (Davis, 2006) and during the observation of threatening stimuli (Davis, 2006; Anokhin and Golosheykin, 2009). Moreover, the observation of fearful faces increases corticospinal motor tract excitability, compared to happy or neutral faces, as revealed by TMS (Schutter et al., 2008). Accordingly, we defined the Fear-DCM by including those areas that could participate in motor representation for action preparation, and we investigated whether the effective connectivity between these areas was specifically modulated by Fear. In particular, we tested the most relevant hypotheses that there should be a Fear-specific increase in connectivity between RBA6 and RPcn/SPL, in

agreement with the role of the fronto-parietal network in action representation, and that there should be an increased effective connectivity of these fronto-parietal regions with the amygdala and the right inferior occipital gyrus.

The results for the Fear-DCM model indicated an increase of connectivity strength for Fear in the connections RIOG->RPcn/SPL, RIOG->RBA6, Ramy->RPcn/SPL, RPcn/SPL->RIOG, RBA6->RIOG, and RBA6->RPcn/SPL. These increases were significantly greater than those for all or a subset of the other three emotions (Table 3A and Figure 2A). Action preparation and action control were hypothesized to depend in particular on the RBA6->RPcn/SPL connection, which was indeed modulated more strongly by Fear than by Sadness and Happiness, thus supporting the idea that action representation and preparation plays a central role in watching and experiencing fearful emotions.

A further interesting set of observations regards the directionality of the significantly modulated connection strengths within Fear DCM. First, it appears that visual information is not conveyed from the RIOG to Ramy in a specific manner for Fear compared to the other emotions, as may have been predicted by models that ascribe a preferential role of the amygdala in fear processing. Specific visual information for Fear is in turn conveyed to both areas of the fronto-parietal network, interestingly with backward, possibly feedback, effects. Second, the RPcn/SPL region appears to assume an integration role in the context of action representation and preparation in reaction to fearful stimuli, as all the other three regions increase their connection strengths toward this area.

4.4. Disgust

In comparison to the other emotions investigated here, Disgust elicited activations within an extensive array of cortical and subcortical structures (Table 2B and Figure 2C). The brain regions usually described as having a predominant role in disgust processing, in

addition to the core emotion brain network, are the insula and the basal ganglia, which have been shown to participate in both disgust recognition and perception (Sprengelmeyer, 2007; Wicker et al., 2003). Other reported disgust-related brain regions include the orbitofrontal cortex, superior frontal gyrus, precentral gyrus, somatosensory areas SI and SII, cingulate cortex, lateral temporal cortex and parietal regions (angular gyrus, and precuneus), visual areas (cuneus, middle occipital and lingual gyri), hypothalamus and cerebellar lobes (Jabbi et al., 2008; Schienle et al., 2006; Trautmann et al., 2009). Altogether, our results were very much consistent with such a pattern, with one main exception, i.e. the lack of disgust-specific activations in the basal ganglia in our study. Using a Small Volume Correction procedure constrained to the caudate, putamen and globus pallidus anatomical regions, we actually found significant activations for Disgust compared to Neutral. However, such an effect cannot be regarded as disgust-specific, as the same statistical procedure yielded basal ganglia activations for the other emotion conditions as well. In fact, this lack of disgust-specificity of the basal ganglia appears to be consistent with previous reports in the literature. More specifically, theories on the perception of disgust have been supported from research concerning Huntington's disease (Sprengelmeyer et al., 1996), Parkinson's disease (Suzuki et al., 2006) and Obsessive-Compulsive disorder (Corcoran et al., 2008), which emphasized the dependence of disgust recognition upon basal ganglia integrity. Other studies, however, have found that recognition impairment in these diseases also extended to other emotional expressions, not only disgust (Kipps et al., 2007; Milders et al., 2003). As a consequence of focal basal ganglia lesions, the neurophysiological response to an implicit processing of disgust, but also of fear, is altered (Paulmann et al. 2009). Accordingly, we did not include the basal ganglia in the DCM analysis, in order not to weaken the specificity of the Disgust-DCM model.

Although disgust has often been described as a guardian of the borders of the bodily self (Fessler and Haley, 2006; Miller, 2004), with the skin having a central role in disgust (Plutchik, 1980), to our knowledge no study yet has investigated the neural correlates of disgust in relation to the sense of one's own bodily state or to somatosensory perception. Consequently, we defined a Disgust-DCM model, which contained the RIOG as an input area, and the connections between the right amygdala, the right thalamus, the left insula and, crucially, the somatosensory cortex. As already noted above, in consideration of the great number of areas by Disgust, the inclusion of only these five brain regions in the Disgust-DCM model reflects a set of compromises due to the technical limitations of the DCM method (see section 2.5.3). In particular, we chose to only include the most relevant areas constituting a somatosensory network mediating bodily representations, namely BA2 and the thalamus, plus the Lins due to its widely known engagement in disgust experience.

We observed stronger modulatory strengths for Disgust with respect to all the other experimental conditions in the following connections (Table 3B and Figure 2B): RIOG->Lins, RIOG->RBA2, Ramy->Lins, Ramy->RBA2, and RBA2->RIOG. Furthermore, watching Disgust scenarios resulted in significantly greater modulatory strengths within RIOG->Ramy and Ramy->RIOG, compared to Fear, Sadness and Neutral video-clips. Crucially, we also found increased connectivity for Disgust compared to Fear, Sadness and Happiness within Lins->RBA2, and compared to Fear and Sadness within Rtha->Lins and RBA2->Lins. In the context of our hypothesis, the Disgust-specific effects in the connections between Lins and RBA2 take a particularly relevant position. Both these regions receives modulatory input from visual cortices and the amygdala, whose activity is supposed to be related to stimulus salience. These connections may constitute the input necessary for a bodily representation that represents part of the response to disgusting stimuli. Moreover, the reciprocal interactions between insula and somatosensory cortices

are particularly relevant because they suggest that the perception of the body and the self is enhanced in the experience of disgust.

4.5. Sadness

Sadness has been previously associated with brain structures overlapping with those involved in happiness, i.e. the medial prefrontal cortex and portions of the anterior cingulate cortex (Phan et al., 2002). In another study, passive viewing of sad films elicited a much larger network of brain regions, including the inferior frontal gyrus, middle and superior temporal gyri, insula, medial precuneus, lingual gyrus, amygdala and thalamus (Goldin et al., 2005). In our study, many of these brain regions were either found to be conjointly activated by all emotions (Table 1A) or specifically (possibly, significantly more) activated by other emotions than Sadness (Tables 2A,B,D). We did not find any Sadness-specific effects with the specified exclusively masked contrasts and significance threshold, even when restricting the analysis to a small volume centered on the medial prefrontal cortex (based on Murphy et al., 2003), according to our common a priori hypothesis for Sadness and Happiness. However, these results must not be taken as evidence of an altogether lack of activation for Sadness. Clearly, the brain regions highlighted by the conjunction analysis were also active for processing sad stimuli. Our data only showed that there were no additional activations that were specific and unique for Sadness. The lack of significant specific effects may be due to stimulus characteristics. The temporal course of sadness has been defined as slower for sadness than for other emotions, as it gradually rises to peak intensity in response to sad films in a much slower and smoother temporal evolution compared to other emotions (Goldin et al., 2005). Since the stimuli presented in this study were relatively brief, it may be the case that the time necessary to evoke a significant activation may extends in a time window that exceeded that of the current study.

In addition to these stimulus characteristics, it may be possible that other activations in addition to those shown by the conjunction analysis may have been elicited by Sadness in an overlapping manner with those of a subset of the other emotions, in particular those induced by Happiness. In an ad-hoc analysis, we therefore looked for specific effects shared by both Sadness and Happiness compared to the Neutral baseline (exclusively masking by (F-N) and (D-N)). Significant activations were found in the right inferior frontal gyrus and in the right middle temporal gyrus (data not shown). Conforming to our stringent criteria of specificity to a particular emotion, however, we decided not to investigate these brain regions further with Dynamic Causal Modeling.

4.6. Happiness

Happiness is a complex process that often involves reward processing (Rolls, 2000) and enjoyable activities (Koepp et al., 1998). It is quite different from simple amusement, which is much more used in affective research (Rottenberg et al., 2007). The scenes depicted in the short films for the Happiness condition were meaningful interactions among subjects, which had to be decoded in order to understand the joyful emotional content. The Happiness-specific effects found here included the left and right middle temporal gyrus (STS), the right superior temporal gyrus (RTPJ), and the right superior medial frontal gyrus (RMPFC) (Table 2D and Figure 1D). These findings are in good agreement with the literature, although previous report did not point out a specificity of these brain regions for happiness. Superior temporal gyrus activations have been found for conditions of viewing amusing films compared to neutral (Goldin et al., 2005), together with MPFC activations that were slightly more dorsally located compared to our study. Similar temporal activations for happiness were also reported by Trautmann and colleagues (2009) in comparing dynamic to static expressions: in their study, an STS involvement was also found for disgust. STS and TPJ activations were also described by Lee and Siegle (in

press), but were referred to the evaluation of others' emotions in general, not to a discrete emotional category.

The MPFC has also not been specifically ascribed to happiness, but rather to cognitive aspects common to all emotions, as appraisal processes or interpretation of emotions (Phan et al., 2002). A recent work of functional connectivity described a network consisting of MPFC and STS as involved in reasoning about others' mental states during thinking about scenarios of social emotions (Burnett and Blakemore, 2009). This connection was engaged more for social emotions than for disgust and fear scenarios. The MPFC also participates in processes like extinction learning and emotional regulation (Quirk et al., 2003; Maren and Quirk, 2004; Milad et al., 2005), possibly providing an inhibitory input to the amygdala. A meta-analysis by Murphy and colleagues (2003) found happiness-related activations in the supracallosal anterior cingulate cortex and in the dorsomedial prefrontal cortex, with comparable coordinates to those reported here. These meta-analysis effects were also found for sadness at a comparable significance level.

Based on these findings and those of the present conjunction analysis, we defined a DCM model including the right inferior occipital gyrus, the right amygdala, the RTPJ and RMPFC, following the hypothesis that the functional integration between the areas of this neural network subserving mentalising and representation of others' mental states would be stronger during watching Happiness situations depicting the interaction among conspecifics than during the observation of aggression (Fear) or contamination (Disgust) scenarios. These processes may be central in the recognition of happiness which requires a more cognitive-demanding evaluation of the stimuli. In particular, the process of reasoning about others' mental states outlined above was hypothesized to depend more strongly on the functional integration between RTPJ and RMPFC.

Our results showed that watching scenes of Happiness resulted in an increase of the connectivity strength on RTPJ from the other three brain regions included in the model

(RIOG, Ramy, and RMPFC). Of particular relevance for the specified Happiness-DCM model is the fact that we found stronger modulatory strength for the connection RMPFC->RTPJ, with respect to watching scenes of Fear or Disgust (Table 3C and Figure 2C). These data point to the temporo-parietal junction as a site of integration of emotionally-loaded sensory information together with the appraisal and interpretive processes mediated by the medial prefrontal cortex.

It is interesting to note that also in the Happiness-DCM no significant backward modulations reached the right amygdala, a feature shared with the other two specified models (Fear-DCM and Disgust-DCM). Thus, the right amygdala appears to only induce forward modulations to content-specific brain regions in the context of the particular model-relevant emotion (RPcn/SPL for Fear; RBA2 and Lins for Disgust; RTPJ for Happiness). This may imply that the amygdala is capable of exerting a modulatory role with respect to polymodal higher order cortical regions that process cognitive, sensorimotor and somatosensory aspects of emotions, and thus to exert an homeostatic regulation of behavior in response to the quality of the induced emotional experience.

Finally, it is important to note that none of the connections withing Happiness-DCM were significantly stronger for Happiness compared to Sadness, even if the areas defined in the model were extracted from the analysis of Happiness specific effects. This may imply that even if Sadness did not elicit significant specific activation, these areas may play a role also in this condition, in line with the already mentioned meta-analysis (Murphy et al., 2003).

5. CONCLUSION

We investigated the neural responses associated with four film-induced emotions representing different basic affective systems and examined the effective connectivity within the networks linking the neural structures involved in emotions. Both neural

similarities and differences emerged, showing that, at least in women, emotions could be organized in the brain as basic neural systems that share some structures for the processing of the emotional salience and differ with respect to the specific sensorimotor, somatosensory, and cognitive components involved by each kind of emotion. In particular, the effective connectivity analysis indicated that core regions involved in emotion processing interact with content-specific brain regions to generate multi-componential affective responses. Our results indicate that emotions are complex events that modulate specialized distributed neural patterns through which the information can be processed, integrated, and modulated, so as to regulate psychological and behavioral activity on the basis of emotion. The emotional response derives from the combination of domain-general and domain-specific processes, and the functional integration of both these aspects instantiates the full emotional experience.

6. FUNDING

This work was supported by the European Community (“BRAINTUNING” – STREP FP6-2004-NEST-PATH-IMP).

7. REFERENCES

Adolphs R. 2002. Recognizing emotion from facial expressions: Psychological and neurological mechanisms. Behav Cogn Neurosci Rev. 1:21-62.

Ambadar Z, Schooler J, Cohn J. 2005. Deciphering the enigmatic face. Psychol Sci. 16:403–410.

Anokhin AP, Golosheykin S. 2009. Startle modulation by affective faces. Biol Psychol. 83:37-40.

Atkinson A, Heberlein A, Adolphs R. 2007. Spared ability to recognise fear from static and moving whole-body cues following bilateral amygdala damage. Neuropsychologia. 45:2772–2782.

Benjamini Y, Hochberg Y. 1995. Controlling the false discovery rate: a practical and powerful approach to multiple testing. J Roy Stat Soc B Met. 57:289–300.

Boucher JD. 1983. Antecedents to emotions across cultures. In: Irvine SH, Berry JW, editors. Human assessment and cultural factors. New York: Plenum. p 407–420.

Breiter HC, Etcoff NL, Whalen PJ, Kennedy WA, Rauch SL, Buckner RL, Strauss MM, Hyman SE, Rosen BR. 1996. Response and habituation of the human amygdala during visual processing of facial expression. Neuron. 17:875–888.

Burnett S, Blakemore S. 2009. Functional connectivity during a social emotion task in adolescents and in adults. Eur J Neurosci. 29:1294-1301.

Calvo-Merino B, Glaser D, Grèzes J, Passingham R, Haggard P. 2005. Action Observation and Acquired Motor Skills: An fMRI Study with Expert Dancers. Cereb Cortex. 15:1243-1249.

Corcoran K, Woody S, Tolin D. 2008. Recognition of facial expressions in obsessive–compulsive disorder. J Anxiety Disord. 22:56–66.

Davis M. 2006. Neural systems involved in fear and anxiety measured with fear-potentiated startle. Am Psychol. 61:741–756.

Decety J, Grèzes J. 2006. The power of simulation: imagining one's own and other's behavior. Brain Res. 1079:4–14.

de Gelder B, Snyder J, Greve D, Gerard G, Hadjikhani N. 2004. Fear fosters flight: A mechanism for fear contagion when perceiving emotion expressed by a whole body. Proc Nat Acad Sci USA. 101:16701-16706.

Dolan R, Fletcher P, Morris J, Kapur N, Deakin J, Frith C. 1996. Neural activation during covert processing of positive emotional facial expressions. Neuroimage 4:194–200.

Eimer M, Holmes A. 2007. Event-related brain potential correlates of emotional face processing. Neuropsychologia. 45:15–31.

Ekman P. 1999. Basic emotions In: Dalgleish T, Power MJ, editors. Handbook of cognition and emotion. New York: John Wiley & Sons. p 45–60.

Ethofer T, Anders S, Wiethoff S, Erb M, Herbert C, Saur R, Grodd W, Wildgruber D. 2006. Effects of prosodic emotional intensity on activation of associative auditory cortex. NeuroReport 17:249-253.

Ethofer T, Van De Ville D, Scherer K, Vuilleumier P. 2009. Decoding of Emotional Information in Voice-Sensitive Cortices. Curr Biol. 19:1028-1033.

Feldman Barrett L, Mesquita B, Ochsner K, Gross J. 2007. The experience of emotion. Annu Rev Psychol. 58:373–403.

Fessler D, Haley K. 2006. Guarding the perimeter: The outside-inside dichotomy in disgust and bodily experience. Cogn Emot. 20:3–19.

Flykt A. 2006. Preparedness for action: Responding to the snake in the grass. Am J Psychol. 119:29–43.

Freese JL, Amaral DG. 2005. The organization of projections from the amygdala to visual cortical areas TE and V1 in the macaque monkey. J Comp Neurol 486:295-317.

Frijda NH. 1986. The emotions. Cambridge, UK: Cambridge University Press.

Friston K, Harrison L, Penny W. 2003. Dynamic causal modelling. Neuroimage. 19:1273–1302.

Galati D, Sciaky R. 1995. The Representation of Antecedents of Emotions in Northern and Southern Italy: A Textual Analysis. J Cross Cult Psychol. 26:123-140.

Goldin PR, Hutcherson CA, Ochsner KN, Glover GH, Gabrieli JD, Gross JJ. 2005. The neural bases of amusement and sadness: A comparison of block contrast and subject-specific emotion intensity regression approaches. Neuroimage. 27:26–36.

Gray JA. 1994. Three fundamental emotion systems. In: Ekman P, Davidson R, editors. The nature of emotion: Fundamental questions. New York: Oxford University Press. p 243–247.

Grèzes J, Pichon S, de Gelder B. 2007. Perceiving fear in dynamic body expressions. Neuroimage. 35:959–967.

Guillot A, Collet C, Nguyen V, Malouin F, Richards C, Doyon J. 2008. Brain activity during visual versus kinesthetic imagery: An fMRI study. Hum Brain Mapp. 30:2157-2172.

Hanakawa T, Immisch I, Toma K, Dimyan M, Van Gelderen P, Hallett M. 2003. Functional properties of brain areas associated with motor execution and imagery. J Neurophysiol. 89:989-1002.

Heath RG, Cox AW, Lustick LS. 1974. Brain Activity During Emotional States. Am J Psychiatry 131:858-862.

Heath RG, Dempesy CW, Fontana CJ, Myers WA. 1978. Cerebellar stimulation: effects on septal region, hippocampus, and amygdala of cats and rats. Biol Psychiatry 13:501-529.

Hutcherson CA, Goldin PR, Ochsner KN, Gabrieli JD, Barrett LF, Gross JJ. 2005. Attention and emotion: Does rating emotion alter neural responses to amusing and sad films? Neuroimage. 27:656–668.

Jabbi M, Bastiaansen J, Keysers C. 2008. A common anterior insula representation of disgust observation, experience and imagination shows divergent functional connectivity pathways. PLoS One. 3:e2939-2947.

Kipps CM, Duggins AJ, McCusker EA, Calder AJ. 2007. Disgust and happiness recognition correlate with anteroventral insula and amygdala volume respectively in preclinical Huntington's disease. J Cogn Neurosci. 19:1206–1217.

Koepp M, Gunn R, Lawrence A, Cunningham V, Dagher A, Jones T, Brooks D, Bench C, Grasby P. 1998. Evidence for striatal dopamine release during a video game. Nature. 393:266–267.

Lane R, Fink G, Chau P, Dolan R. 1997. Neural activation during selective attention to subjective emotional responses. Neuroreport. 8:3969-3972.

Lang P, Bradley M, Cuthbert B. 1997. International affective picture system. IAPS. : Technical manual and affective ratings. NIMH Center for the Study of Emotion and Attention, Gainesville FL.

Lang PJ, Bradley MM, Fitzsimmons JR, Cuthbert BN, Scott JD, Moulder B, Nangia V. 1998. Emotional arousal and activation of the visual cortex: an fMRI analysis. Psychophysiology. 35:199-210.

LeDoux JE. 2000. Emotion Circuits in the Brain. Annu Rev Neurosci 23:155-184.

Lee KH, Siegle GJ. in press. Common and distinct brain networks underlying explicit emotional evaluation: a meta-analytic study. Soc Cogn Affect Neurosci. doi:10.1093/scan/nsp001.

Liu L, Ioannides A, Streit M. 1999. Single trial analysis of neurophysiological correlates of the recognition of complex objects and facial expressions of emotion. Brain Topogr. 11:291–303.

Loughead J, Gur RC, Elliott M, Gur RE. 2007. Neural circuitry for accurate identification of facial emotions. Brain Res. 1194:37-44.

MacLean P. 1949. Psychosomatic disease and the "visceral brain": Recent developments bearing on the Papez theory of emotion. Psychosom Med. 11:338-353.

MacLean P. 1952. Some psychiatric implications of physiological studies on frontotemporal portion of limbic system. visceral brain. . Electroen Clin Neuro. 4:407–418.

MacLean, P. 1970. The triune brain, emotion, and scientific bias. In Schmidt FO, editor. The neurosciences. Second study program. New York:Rockefeller University Press. p 336-349.

Malouin F, Richards CL, Jackson PL, Dumas F, Doyon J. 2003. Brain activations during motor imagery of locomotor-related tasks: A PET study. Hum Brain Mapp. 19:47-62.

Maren S, Quirk GJ. 2004. Neuronal signalling of fear memory. Nature Rev Neurosci. 5:844–852.

Mayberg HS, Liotti M, Brannan SK, McGinnis S, Mahurin RK, Jerabek PA, Silva JA, Tekell JL, Martin CC, Lancaster JL, Fox PT. 1999. Reciprocal Limbic-Cortical Function and Negative Mood: Converging PET Findings in Depression and Normal Sadness. Am J Psychiatry. 156:675-682.

Middleton FA, Strick PL. 2001. Cerebellar Projections to the Prefrontal Cortex of the Primate. J Neurosci. 21:700-712.

Milad MR, Quinn BT, Pitman RK, Orr SP, Fischl B, Rauch SL. 2005. Thickness of ventromedial prefrontal cortex in humans is correlated with extinction memory. Proc Nat Ac Sci USA. 102:10706-10711.

Milders M, Crawford J, Lamb A, Simpson S. 2003. Differential deficits in expression recognition in gene-carriers and patients with Huntington's disease. Neuropsychologia. 41:1484–1492.

Miller S. 2004. Disgust: The gatekeeper emotion. Hillsdale, NJ: The Analytic Press. 213 p.

Morris J, Friston K, Buchel C, Frith C, Young A, Calder A, Dolan R. 1998. A neuromodulatory role for the human amygdala in processing emotional facial expressions. Brain. 121:47-57.

Morris J, Öhman A, Dolan R. 1999. A subcortical pathway to the right amygdala mediating “unseen” fear. Proc Nat Acad Sci USA. 96:1680-1685.

Morris J, DeBonis M, Dolan R. 2002. Human amygdala responses to fearful eyes. Neuroimage. 17:214–222.

Murphy FC, Nimmo-Smith I, Lawrence AD. 2003. Functional neuroanatomy of emotions: a meta-analysis. Cogn Affect Behav Neurosci. 3:207–233.

Oldfield R. 1971. The assessment and analysis of handedness: The Edinburgh inventory. Neuropsychologia. 9:97-113.

Panksepp J. 2008. The affective brain and core-consciousness: How does neural activity generate emotional feelings In: Lewis M ; Haviland-Jones JM, Barrett L Feldman, editors. Handbook of emotions. New York: The Guildford Press. p 47–67.

Paulmann S, Pell MD, Kotz SA. 2009. Comparative processing of emotional prosody and semantics following basal ganglia infarcts: ERP evidence of selective impairments for disgust and fear. Brain Res. 1295:159-169.

Pessoa L. 2008. On the relationship between emotion and cognition. Nat Rev Neurosci. 9:148–158.

Phan K, Wager T, Taylor S, Liberzon I. 2002. Functional neuroanatomy of emotion: a meta-analysis of emotion activation studies in PET and fMRI. Neuroimage. 16:331–348.

Phan KL, Wager TD, Taylor SF, Liberzon I. 2004. Functional neuroimaging studies of human emotions. CNS Spectr. 9:258–266.

Phelps E, LeDoux J. 2005. Contributions of the amygdala to emotion processing: from animal models to human behavior. Neuron. 48:175–187.

Plutchik R. 1980. Emotion: A psychoevolutionary synthesis. New York: Harper & Row.

Quirk GJ, Likhtik E, Pelletier JG, Pare D. 2003. Stimulation of Medial Prefrontal Cortex Decreases the Responsiveness of Central Amygdala Output Neurons. J Neurosci. 23:8800-8807.

Rolls ET. 2000. On the brain and emotion. Behav Brain Sci. 23:219–228.

Roebroeck A, Formisano E, Goebel R. 2005. Mapping directed influence over the brain using Granger causality and fMRI. Neuroimage. 25(1): 230-242.

Rottenberg J, Ray R, Gross J. 2007. Emotion elicitation using films. In: Coan JA and Allen JB, editors. The handbook of emotion elicitation and assessment New York: Oxford University Press. p 9–28.

Scherer K. 1988. Criteria for emotion-antecedent appraisal: A review. In: Hamilton V ; Bower GH, Frijda NH, editors. Cognitive perspectives on emotion and motivation. New York: Kluver Academic Plenum Publishers. p 89–126.

Scherer K. 2000. Emotions as episodes of subsystem synchronization driven by nonlinear appraisal processes. In: Lewis MD, Granic I, editors. Emotion, development, and self-organization: Dynamic systems approaches to emotional development. Cambridge: Cambridge University Press. p 70–99.

Schienle A, Schäfer A, Hermann A, Walter B, Stark R, Vaitl D. 2006. fMRI responses to pictures of mutilation and contamination. Neurosci Lett. 393:174–178.

Schmahmann J, Sherman J. 1998. The cerebellar cognitive affective syndrome. Brain 121:561-579.

Schutter DJLG, Hofman D, Van Honk J. 2008. Fearful faces selectively increase corticospinal motor tract excitability: a transcranial magnetic stimulation study. Psychophysiol. 45:345-348.

Shuler MG, Bear MF. 2006. Reward Timing in the Primary Visual Cortex. Science 311:1606-1609.

Sprengelmeyer R, Young A, Calder A, Karnat A, Lange H, Homberg V, Perrett D, Rowland D. 1996. Loss of disgust: perception of faces and emotions in Huntington's disease. Brain. 119:1647-1665.

Sprengelmeyer R. 2007. The neurology of disgust. Brain. 130:1715-1717.

Stark R, Zimmermann M, Kagerer S, Schienle A, Walter B, Weygandt M, Vaitl D. 2007. Hemodynamic brain correlates of disgust and fear ratings. Neuroimage 37:663–673.

Stephan KE, Penny WD, Moran RJ, den Ouden HEM, Daunizeau J, Friston KJ. 2010. Ten simple rules for dynamic causal modeling. Neuroimage 49(4):3099-3109.

Streit M, Ioannides A, Liu L, Wölver W, Dammers J, Gross J, Gaebel W, Müller-Gärtner H. 1999. Neurophysiological correlates of the recognition of facial expressions of emotion as revealed by magnetoencephalography. Cogn Brain Res. 7:481-491.

Suzuki A, Hoshino T, Shigemasu K, Kawamura M. 2006. Disgust-specific impairment of facial expression recognition in Parkinson's disease. Brain. 129:707-717.

Trautmann SA, Fehr T, Herrmann M. 2009. Emotions in motion: Dynamic compared to static facial expressions of disgust and happiness reveal more widespread emotion-specific activations. Brain Res. 1284:100–115.

Tsuchiya N, Moradi F, Felsen C, Yamazaki M, Adolphs R. 2009. Intact rapid detection of fearful faces in the absence of the amygdala. Nat Neurosci. 12:1224.

Vuilleumier P, Armony J, Driver J, Dolan R. 2003. Distinct spatial frequency sensitivities for processing faces and emotional expressions. Nat Neurosci. 6:624–631.

Vuilleumier P, Richardson MP, Armony JL, Driver J, Dolan RJ. 2004. Distant influences of amygdala lesion on visual cortical activation during emotional face processing. Nat Neurosci 7:1271-1278.

Wager TD, Phan K, Liberzon I, Taylor SF. 2003. Valence, gender, and lateralization of functional brain anatomy in emotion: a meta-analysis of findings from neuroimaging. Neuroimage. 19:513-531.

Wager T, Barrett L, Bliss-Moreau E, Lindquist K, Duncan S, Kober H, Joseph J, Davidson M, Mize J. 2008. The neuroimaging of emotion. In: Lewis M, Haviland-Jones JM, Barrett L Feldman, editors. The handbook of emotion. New York: The Guildford Press. p 249-271.

Weyers P, Mühlberger A, Hefele C, Pauli P. 2006. Electromyographic responses to static and dynamic avatar emotional facial expressions. Psychophysiol. 43:450–453.

Wicker B, Keysers C, Plailly J, Royet J, Gallese V, Rizzolatti G. 2003. Both of Us Disgusted in My Insula The Common Neural Basis of Seeing and Feeling Disgust. Neuron. 40:655–664.

TABLES

Table 1. Results of the null conjunction analysis performed on the contrasts between each emotional condition and the Neutral condition [(H-N) conj. (F-N) conj. (D-N) conj. (S-N)] (P<0.05, FWE corrected at whole brain level, or Small Volume Corrected where indicated by an asterisk). §According to www.fz-juelich.de/ime/spm_anatomy_toolbox.

	Cluster size	Voxel Level		MNI coordinates		
Brain region (cytoarchitectonic probability§)	K (voxels)	Z-score	P-value	x	y	z
Right SupraMarginal Gyrus (Area Pfm 50%)	5	5.01	0.023	56	-40	28
Right PostCentral Gyrus (Area 2 90%)	6	5.00	0.024	30	-40	48
Right Superior Parietal Lobule (Area SPL 50%)	"	5.46	0.002	34	-48	56
Right Inferior Temporal Gyrus	150	6.49	0.000	50	-60	-8
Right Inferior Temporal Gyrus	"	5.70	0.001	46	-40	-20
Right Middle Temporal Gyrus	"	5.73	0.000	54	-60	0
Right Inferior Occipital Gyrus	"	5.90	0.000	44	-72	-16
Right Inferior Occipital Gyrus (Area hOC4v (V4) 60%)	"	4.87	0.048	36	-80	-16
Right Cerebellum(VI)	"	5.65	0.000	42	-60	-24
Right Amygdala (Area SF 70%)	56	3.68	0.018 *	22	-4	-20
Left Superior Parietal Lobule (Area SPL 7PC 60%)	5	4.99	0.026	-36	-50	60
Left Fusiform Gyrus	20	5.08	0.016	-44	-62	-20
Left Inferior Occipital Gyrus (Area hOC4v (V4) 50%)	"	5.48	0.002	-42	-84	-12

Table 2A. Specific activations for the (F – N) contrast [(exclusively masked by (H – N), (D – N), and (S – N)] (P<0.05, FWE corrected). §According to www.fz-juelich.de/ime/spm_anatomy_toolbox.

	Cluster size	Voxel Level		MNI coordinates		
Brain region (cytoarchitectonic probability§)	K (voxels)	Z-score	P-value	x	y	z
Right Superior Frontal Gyrus (Area 6 30%)	13	5.82	0.000	24	-6	60
Right Superior Parietal Lobule (Area SPL 7PC 60%)	183	5.90	0.000	24	-52	68
Right Precuneus (Area SPL 5L 50%)	"	7.68	0.000	10	-60	68
Right Fusiform Gyrus	44	6.76	0.000	28	-64	-8
Right Fusiform Gyrus (Area hOC4v (V4) 90%)	"	5.15	0.011	28	-74	-8
Right Lingual Gyrus (Area 18 80%)	14	5.63	0.001	18	-84	-12
Right Middle Occipital Gyrus	148	7.19	0.000	44	-76	12
Right Superior Occipital Gyrus	"	6.11	0.000	24	-90	16
Left Precuneus (Area SPL 7A 70%)	61	7.07	0.000	-16	-58	60
Left Fusiform Gyrus (Area hOC4v (V4) 60%)	11	5.23	0.007	-22	-76	-12
Left Lingual Gyrus (Area hOC4v (V4) 70%)	10	5.64	0.001	-20	-82	-16
Left Middle Occipital Gyrus	10	6.64	0.000	-40	-82	20

Table 2B. Specific activations for the (D – N) contrast [(exclusively masked by (H – N), (F – N), and (S – N)] (P<0.05, FWE corrected). §According to www.fz-juelich.de/ime/spm_anatomy_toolbox.

	Cluster size	Voxel Level		MNI coordinates		
Brain region (cytoarchitectonic probability§)	K (voxels)	Z-score	P-value	x	y	z
Right Inferior Frontal Gyrus (pars triangularis, Area 45 50%)	17	5.64	0.001	52	38	12
Right Inferior Frontal Gyrus (pars opercularis, Area 44 40%)	39	6.82	0.000	58	8	24
Right Precentral Gyrus (Area 6 60%)	"	5.00	0.025	56	6	40

Right Postcentral Gyrus (Area 1 70%)	265	4.96	0.030	42	-36	60
Right Postcentral Gyrus (Area 2 60%)	"	7.23	0.000	52	-22	40
Right Postcentral Gyrus (Area PFt 50%)	"	6.73	0.000	42	-30	40
Right Inferior Parietal Lobule (Area 2 70%)	"	6.45	0.000	42	-36	48
Right Angular Gyrus (Area PGp 90%)	8	5.16	0.010	46	-66	36
Right Inferior Temporal Gyrus	15	6.33	0.000	50	-44	-16
Right Precuneus	479	6.60	0.000	12	-56	20
Right Cuneus	"	7.63	0.000	8	-76	32
Right Lingual Gyrus (Area 18 70%)	"	5.16	0.010	12	-50	0
Right Calcarine Gyrus	"	6.39	0.000	8	-60	12
Right Cerebellum (Crus 1)	93	6.96	0.000	28	-76	-32
Right Cerebellum (Crus 2)	"	5.18	0.010	10	-78	-32
Right Cerebellum (VI)	"	5.47	0.002	22	-72	-28
Right Amygdala (Area LB 70%)	14	5.96	0.000	24	-2	-24
Right Thalamus	33	6.42	0.000	14	-8	12
Left Middle Orbito-Frontal Gyrus	41	6.00	0.000	-2	48	-8
Left Superior Medial Frontal Gyrus	6	5.10	0.015	0	58	4
Left Inferior Frontal Gyrus (pars triangularis, Area 45 70%)	52	5.87	0.000	-50	36	20
Left Inferior Frontal Gyrus (pars opercularis, Area 44 50%)	29	5.41	0.003	-56	12	24
Left Precentral Gyrus (Area 6 60%)	"	5.55	0.001	-60	4	32
Left Superior Frontal Gyrus	18	5.53	0.001	-24	60	4
Left Insula Lobe	22	5.72	0.000	-38	-6	8
Left Middle Cingulate Cortex	19	5.44	0.002	0	-38	52
Left Postcentral Gyrus (Area 1 60%)	220	5.73	0.000	-56	-26	48
Left Postcentral Gyrus (Area 2 80%)	"	7.42	0.000	-46	-26	40
Left Postcentral Gyrus (Area PFop 80%)	"	>8	0.000	-60	-22	24
Left Inferior Parietal Lobule	"	7.61	0.000	-46	-40	44
Left Inferior Parietal Lobule (Area hIP2 50%)	"	6.77	0.000	-42	-42	36
Left Angular Gyrus (Area PGa 60%)	49	6.02	0.000	-50	-62	44
Left Hippocampus (Area CA 50%)	8	5.19	0.009	-32	-18	-12
Left Inferior Temporal Gyrus	7	5.98	0.000	-52	-46	-20
Left Middle Temporal Gyrus	8	5.37	0.003	-66	-30	-8
Left Superior Temporal Gyrus	5	5.16	0.011	-56	2	-4
Left Precuneus	479	5.42	0.003	-2	-64	32
Left Cuneus	"	6.91	0.000	-8	-78	28
Left Lingual Gyrus	"	5.14	0.000	-12	-50	0

(Area 18 70%)						
Left Calcarine Gyrus	"	6.72	0.000	-12	-66	12
Left Middle Occipital Gyrus (Area Pgp 70%)	11	5.46	0.002	-44	-74	32
Left Middle Occipital Gyrus	29	6.11	0.000	-28	-72	32
Left Superior Occipital Gyrus	"	5.57	0.000	-24	-74	40
Left Cerebellum(Crus 1)	39	6.22	0.000	-6	-82	-20
Left Cerebellum(Crus 2)	"	6.14	0.000	-14	-86	-28
Left Cerebellum (VI)	8	5.79	0.000	-18	-74	-24
Left Amygdala (Area LB 70%)	8	6.02	0.000	-24	-2	-24
Left Thalamus	6	5.27	0.006	-14	-6	1

Table 2C. Specific activations for the (S– N) contrast [(exclusively masked by (H – N), (F – N), and (D – N)] (P<0.05, FWE corrected). §According to www.fz-juelich.de/ime/spm_anatomy_toolbox.

	Cluster size	Voxel Level		MNI coordinates		
Brain region (cytoarchitectonic probability§)	K (voxels)	Z-score	P-value	x	y	z
No specific activations						

Table 2D. Specific activations for the (H – N) contrast [exclusively masked by (F – N), (D – N), and (S – N)] (P<0.05, FWE corrected at whole brain level, or Small Volume Corrected where indicated by an asterisk). §According to www.fz-juelich.de/ime/spm_anatomy_toolbox.

	Cluster size	Voxel Level		MNI coordinates		
Brain region (cytoarchitectonic probability§)	K (voxels)	Z-score	P-value	x	y	z
Right Superior Medial Frontal Gyrus	36	5.05	0.000 *	4	58	16
Right Middle Temporal Gyrus / Superior temporal sulcus	31	5.80	0.000	54	-42	8
Right Superior Temporal Gyrus / Temporo-parietal junction	5	6.57	0.000	64	-46	12
Left Middle Temporal Gyrus	66	5.96	0.000	-56	-48	8

Table 3A. Significant modulatory effects for the Fear-DCM model (P<0.05, FDR corrected for multiple comparisons). Only the connections displaying a significant one-sample T-Test for Fear are reported; therein, we only list the other conditions yielding significant one-sample and/or paired T-Tests. NS: not significant.

Connection	***One-sample T-Test***		***Paired T-Test***	
	Condition	***(P-value)***	***Contrast***	***(P-value)***
RIOG->RPcn/SPL				
	F	0.0000001929		
	D	NS	F-D	0.00004070
	S	NS	F-S	0.00008786
	H	NS	F-H	0.00003232
	N	NS	F-N	0.000005636
RIOG->RBA6				
	F	0.0000001136		
	D	0.003677	D-S	NS
	S	NS	F-S	0.0002709
	H	NS	F-H	0.001182
	N	NS	F-N	0.00001428
RAmy->RPcn/SPL				
	F	0.004541		
	H	NS	F-H	0.005548
RPcn/SPL->RIOG				
	F	0.00003852		
	S	NS	F-S	0.003447
	H	NS	F-H	0.000345
RBA6->RIOG				
	F	0.002927		
	D	0.000716	F-D	NS
	S	NS	F-S	0.002278
	H	NS	F-H	0.001806
RBA6->RPcn/SPL				
	F	0.001200		
	D	NS	F-D	NS
	S	NS	F-S	0.002289
	H	NS	F-H	0.004116
	N	NS	F-N	0.005413

Table 3B Significant modulatory effects for the Disgust-DCM model (P<0.05, FDR corrected for multiple comparisons). Values in red font represent negative modulatory effects. Only the connections displaying a significant one-sample T-Test for Disgust are reported; therein, we only list the other conditions yielding significant one-sample and/or paired T-Tests. NS: not significant.

Connection	***One-sample T-Test***		***Paired T-Test***	
	Condition	***(P-value)***	***Contrast***	***(P-value)***
RIOG->Ramy				
	D	0.004557		
	F	NS	D-F	0.001765
	S	NS	D-S	0.004727
	H	0.000339	D-H	NS
	N	0.000000341	D-N	0.000007207
RIOG->Lins				
	D	0.00003689		
	F	NS	D-F	0.006966
	S	NS	D-S	0.000009423
	H	NS	D-H	0.0000424
	N	0.0007418	D-N	0.000001839
RIOG->RBA2				
	D	0.0000005835		
	F	0.000003439	D-F	0.001217
	S	NS	D-S	0.000002372
	H	NS	D-H	0.000004447
	N	0.0001230	D-N	0.0000006474
Ramy->RIOG				
	D	0.004557		
	F	NS	D-F	0.001765
	S	NS	D-S	0.004727
	H	0.000339	D-H	NS
	N	0.000000341	D-N	0.000007207
Ramy->Lins				
	D	0.0001799		
	F	NS	D-F	0.002521
	S	NS	D-S	0.00003525
	H	NS	D-H	0.00756
	N	NS	D-N	0.002171
Ramy->RBA2				
	D	0.00003248		

	F	NS	D-F	0.007783
	S	NS	D-S	0.00003616
	H	NS	D-H	0.00006991
	N	NS	D-N	0.0006529
Rtha->Lins	D	0.015650		
	F	NS	D-F	0.005280
	S	NS	D-S	0.011600
Lins->RIOG				
	D	0.001389		
	S	NS	D-S	0.0008902
	H	NS	D-H	0.003284
Lins->RBA2				
	D	0.003379		
	F	NS	D-F	0.01344
	S	NS	D-S	0.02144
	H	NS	D-H	0.01812
RBA2->RIOG				
	D	0.000001532		
	F	0.00005669	D-F	0.01049
	S	NS	D-S	0.00002021
	H	NS	D-H	0.00001627
	N	NS	D-N	0.0002605
RBA2->Lins				
	D	0.008145		
	F	NS	D-F	0.005182
	S	NS	D-S	0.01942

Table 3C Significant modulatory effects for the Happiness-DCM model (P<0.05, FDR corrected for multiple comparisons). Values in red font represent negative modulatory effects. Only the connections displaying a significant one-sample T-Test for Happiness are reported; therein, we only list the other conditions yielding significant one-sample and/or paired T-Tests. NS: not significant.

Connection	***One-sample T-Test***		***Paired T-Test***	
	Condition	***(P-value)***	***Contrast***	***(P-value)***
RIOG->RTPJ				
	H	0.0005936		

	F	0.002817	H-F	NS
	D	NS	H-D	0.007796
	N	0.0002965	H-N	0.000002285
Ramy->RTPJ				
	H	0.001268		
	D	NS	H-D	0.0009408
RMPFC->RTPJ				
	H	0.01081		
	F	NS	H-F	0.005199
	D	NS	H-D	0.001485

FIGURE LEGENDS

Figure 1. **Functional localization of the emotion-specific effects**

Significant activations (P < 0.05, FWE corrected for multiple comparisons) are displayed on cortical renderings and on sagittal (x coordinate level in mm) and axial (z coordinate levels in mm) slices of the anatomical image of one of the participants (warped to the MNI coordinate space). (A) Results of the null conjunction analysis, representing the joint activations for the four emotional conditions (F, D, S, H) compared to the control Neutral condition. (B) Activations specific to Fear. (C) Activations specific to Disgust. (D) Activations specific to Happiness.

Figure 2. **Functional integration between the amygdala and emotion-specific sensorimotor, somatosensory, and cognitive systems**

The top row represents the connection patterns of three specified models. The bottom row, in turn, represents the significant condition-specific connection strength modulations (P < 0.05, FDR corrected for multiple comparisons). Significant one-tailed paired T-test contrasts are indicated in abbreviated forms next to the corresponding connections. (A) Fear-DCM model, testing the hypothesis of stronger positive modulatory effects in a brain network subserving action representation for F compared to all the other conditions. (B) Disgust-DCM model, testing the hypothesis of stronger positive modulatory effects in a brain network subserving somatosensory representations for D compared to all the other conditions. (C) Happiness-DCM model, testing the hypothesis of stronger positive modulatory effects in a brain network subserving mentalising and representation of others' mental states, in relation to the processing of H compared to all the other conditions.

RPcn/SPL: right precuneus/superior parietal lobule complex; RBA6: right premotor cortex (BA 6); Rtha: right thalamus; Lins; left insula; RBA2: right somatosensory cortex

(Brodmann's area 2); RIOG: right inferior occipital gyrus; Ramy: right amygdala; RMPFC: right medial prefrontal cortex; RTPJ: right temporo-parietal junction.

Figure 1

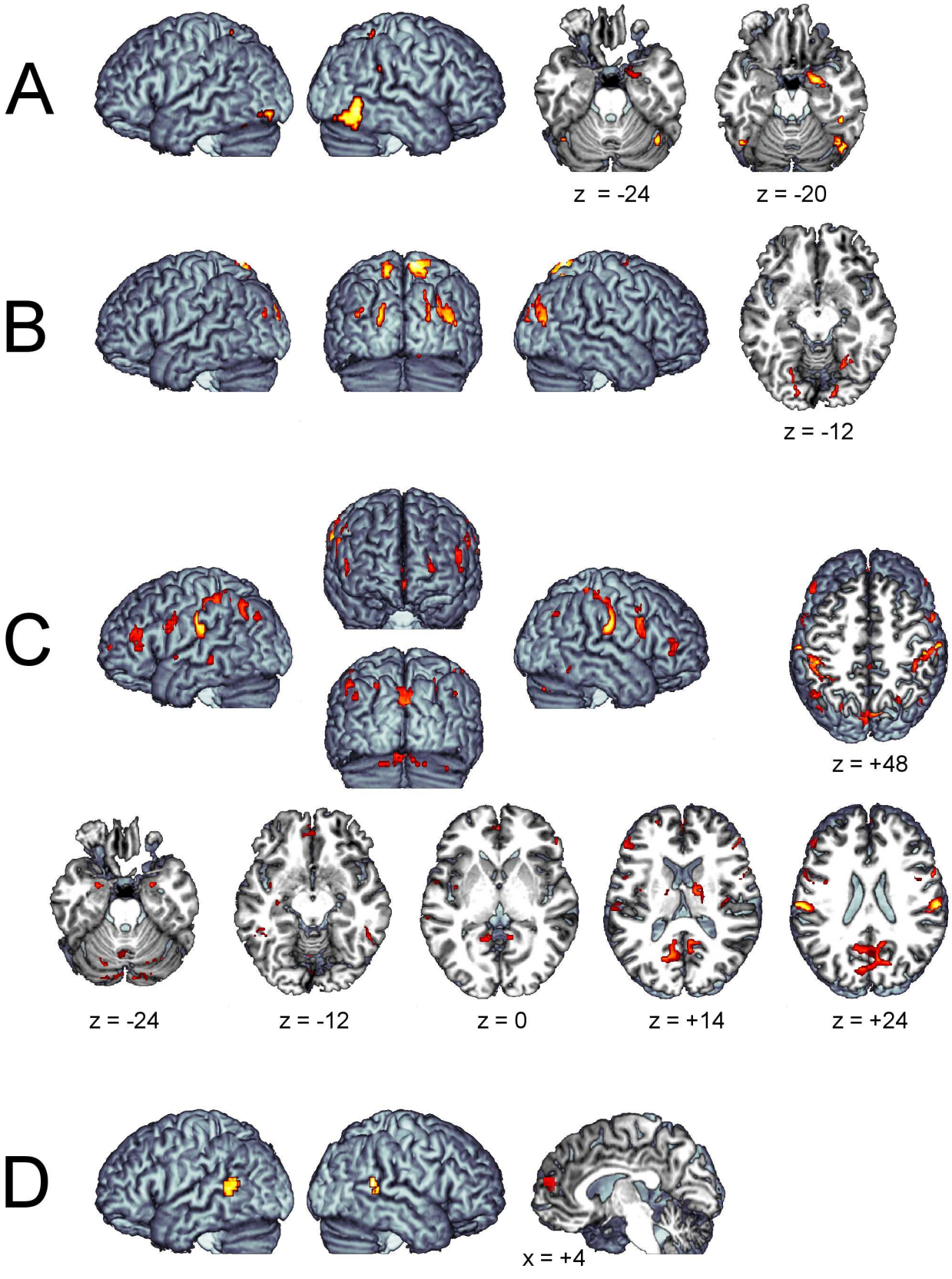

Figure 2

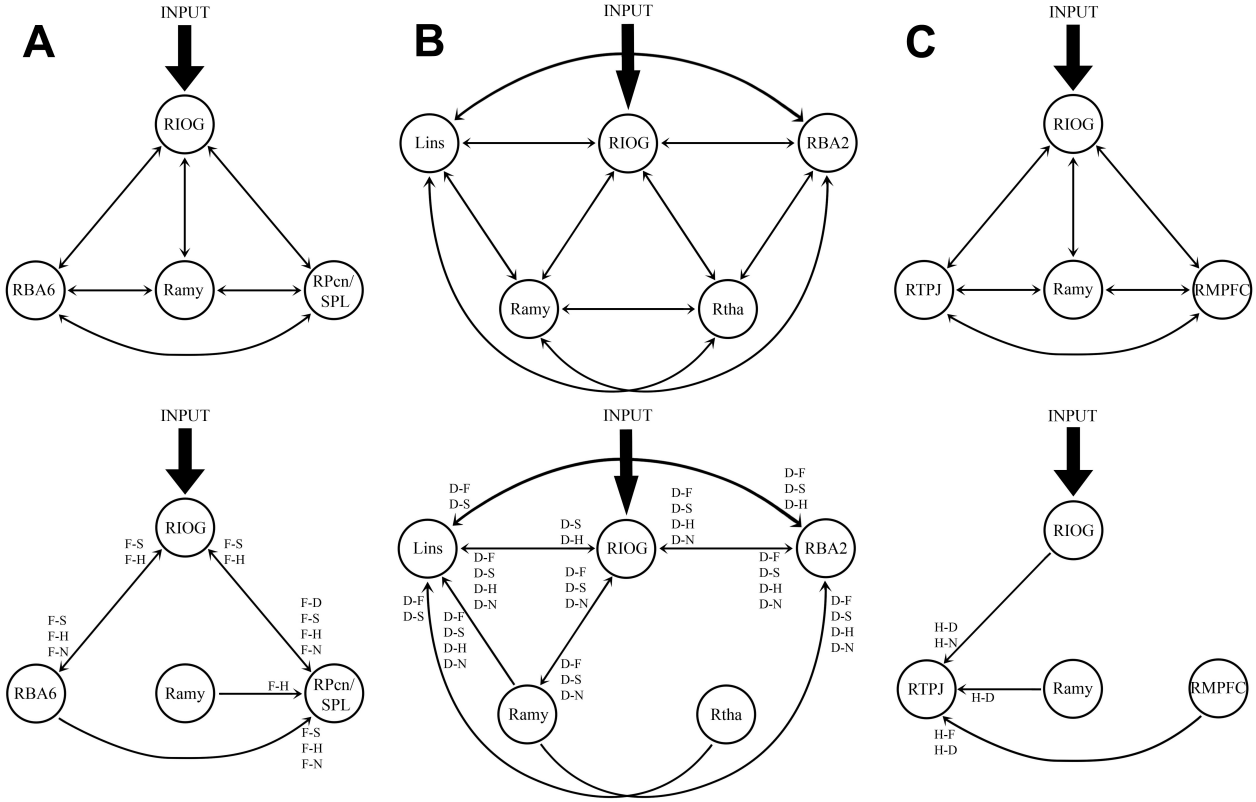
A
INPUT
RIOG
RBA6
Ramy
RPcn/
SPL
B
INPUT
Lins
RIOG
RBA2
Ramy
Rtha
C
INPUT
RIOG
RTPJ
Ramy
RMPFC
INPUT
RIOG
F-S
F-H
F-S
F-H
F-S
F-H
F-N
F-D
F-S
F-H
F-N
RBA6
Ramy
F-H
RPcn/
SPL
F-S
F-H
F-N
INPUT
D-F
D-S
D-S
D-H
D-F
D-S
D-H
D-N
D-F
D-S
D-H
D-N
Lins
RIOG
RBA2
D-F
D-S
D-H
D-N
D-F
D-S
D-H
D-N
D-F
D-S
D-H
D-N
D-F
D-S
D-H
D-N
D-F
D-S
D-N
D-F
D-S
D-N
Ramy
Rtha
INPUT
RIOG
H-D
H-N
RTPJ
H-D
Ramy
RMPFC
H-F
H-D